

Low-energy electron attachment to brominated methanes

Takeyoshi Sunagawa and Hiroshi Shimamori

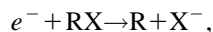
Fukui Institute of Technology, 3-6-1 Gakuen, Fukui 910, Japan

(Received 13 June 1997; accepted 11 August 1997)

The rate constants as a function of the mean electron energy from thermal to about 2 eV at room temperature have been measured for electron attachment to CBr_4 , CHBr_3 , CFBr_3 , CF_2Br_2 , CH_2BrCl , CHBr_2Cl , and CBrCl_3 using the pulse-radiolysis microwave-cavity method combined with microwave heating. The electron attachment cross sections, derived from the rate constant data, all show maximum at zero energy with no noticeable peak at higher electron energies. Based on the differences observed in the absolute magnitude of the cross sections among the brominated compounds as well as those between brominated and the corresponding chlorinated methanes, a model for the dissociative attachment to brominated methanes has been presented. © 1997 American Institute of Physics. [S0021-9606(97)00343-7]

I. INTRODUCTION

Dissociative electron attachment to molecules containing halogen atoms have been widely studied over many years.¹ One of the main target molecules is methanes containing chlorine atom(s) or those with fluorine atoms, since they are used in many practical fields associated with ionized gases as being gaseous dielectrics in high-voltage instrumentation and chemical etchants in plasma processing. They are regarded as key compounds in prevention from ozone layer destruction in the upper atmosphere. From previous studies the following picture has been drawn on the nature of electron attachment to halogenated methanes. In the dissociative electron attachment to a halogenated methane RX ,



where R and X denote a radical and a halogen atom, respectively, the reaction is exothermic when the electron affinity (EA) of X is larger than the dissociation energy (BD) of the R–X bond. Generally, as the exothermicity increases the potential energy for the negative-ion state, which is usually repulsive along the dissociation coordinate, becomes lower, and accordingly the resonance attachment energy becomes lower, leading to a higher probability for low-energy electron attachment. Such a picture is nicely applicable to the dissociative attachment to CF_3X (X=Cl, Br, and I) and CF_2X_2 (X=Cl and Br),² for which the relative magnitude of cross sections in the low-electron-energy region are $\text{CF}_3\text{Cl} < \text{CF}_3\text{Br} < \text{CF}_3\text{I}$ and $\text{CF}_2\text{Cl}_2 < \text{CF}_2\text{Br}_2$. In both series the energy of a carbon- (substituent halogen) antibonding σ^* orbital decreases progressively with successive substitution of heavier halogens. The same interpretation is applicable to the dissociative attachment to chloromethanes, i.e., the rate constants for thermal electron attachment are in the order, $\text{CH}_3\text{Cl} (< 1.9 \times 10^{-15} \text{ cm}^3 \text{ s}^{-1})^3 < \text{CH}_2\text{Cl}_2 (4.7 \times 10^{-12} \text{ cm}^3 \text{ s}^{-1})^4 < \text{CHCl}_3 (2.0 \times 10^{-9} \text{ cm}^3 \text{ s}^{-1})^5 < \text{CCl}_4 (4.0 \times 10^{-7} \text{ cm}^3 \text{ s}^{-1})^5$, where the value of BD for the C–Cl bond decreases with the increase of the number of Cl atoms in the molecule. Perfluorination of chloromethanes enhances the low-energy attachment because the presence of fluorine atom(s) increases the electron affinity of

the parent molecule, thereby pulling down the negative-ion potential closer to the minimum position of the neutral. For other halogenated compounds, especially those containing bromine atoms, one can expect a similar tendency in the magnitude of attachment rates. However, recent measurements for CF_2Br_2 and CFBr_3 indicated that the thermal electron attachment rate constants, 3.0×10^{-7} and $4.8 \times 10^{-9} \text{ cm}^3 \text{ s}^{-1}$,⁶ respectively, do not follow the above expectation. Another difficulty can be found when we compare the rate constants between a chlorinated methane and the corresponding methane substituted with bromine atom(s). The strength of the R–Br bond is usually lower than that of R–Cl bond (the differences ranges from 0.5 to 0.8 eV), while the EA values for both halogen atoms are not much different (3.615 and 3.363 eV for Cl and Br, respectively), so the dissociative electron attachment to brominated methanes may be more exothermic than the corresponding chlorinated methanes. Actually, however, known data for brominated methanes represent an opposite case where the rate constants for thermal electron attachment to CFBr_3 , $4.8 \times 10^{-9} \text{ cm}^3 \text{ s}^{-1}$,⁶ is much lower than that for CFCl_3 , $1.8 \times 10^{-7} \text{ cm}^3 \text{ s}^{-1}$,⁵ in contrast with the cross sections found for dihalogenated methanes as $\text{CF}_2\text{Cl}_2 < \text{CF}_2\text{Br}_2$. A unique character in the electron attachment to brominated methanes can be seen in the unimolecular production of Br_2^- in the thermal electron attachment to CF_2Br_2 and CFBr_3 . Similar processes producing Cl_2^- in chloromethanes (CCl_4 , CH_2Cl_2 , and CFCl_3) occur only at around 1 eV.^{7,8}

Obviously a more systematic study is necessary in order to understand the nature of the electron attachment to brominated methanes. In the present work we have chosen several brominated methanes as well as some methanes in which both chlorine and bromine atoms are included, and the rate constants as a function of the mean electron energy have been measured using the pulse-radiolysis microwave-cavity technique combined with microwave heating.^{5,9} All the obtained data have been converted to cross sections as a function of the electron energy. The effects of the molecular structure and the nature of the substituted atoms on the attachment cross sections are discussed, and a model will be presented to interpret a unique character of the dissociative

attachment to brominated methanes. In the Appendix the cross sections for electron attachment to CCl_4 , CFCl_3 , and CHCl_3 are shown for comparison with those for the brominated methanes.

II. EXPERIMENT

Details of the experimental apparatus and the procedure of measurements were described previously.^{5,9} Briefly, the gas sample comprised of a halogenated compound and Xe as the buffer gas was introduced into a cylindrical quartz cell which was placed in a two-way-mode microwave resonant cavity. The gas was ionized by irradiation of a 3 ns x-ray pulse from Febetron 706. An X-band microwave circuit having a frequency-discriminator unit was used for detection of electron density in the cavity. The outputs were amplified and fed to a storage oscilloscope. The heating microwave power was fed through the cavity to vary the electron temperature. The mean electron energy in the Xe buffer was determined from measured heating power by a procedure described previously.^{5,9}

Xe (>99.999%, Teisan Co.) was used as received. Compounds investigated and their purity are as follows; CBr_4 (99%), CHBr_3 (99+%), CFBr_3 (99+%), CF_2Br_2 (97%), CBrCl_3 (99%), CHBr_2Cl (98%), and CH_2BrCl (99%) supplied by Aldrich. They were used after degassing by freeze-pump-thaw cycles. All the measurements were carried out at room temperature (298 ± 3 K).

In measurements a trace amount of sample compound (lower than 10^{-4} Torr) was added to the 70 Torr Xe buffer, and at a given heating power the lifetimes were measured for the first-order decay of electrons due to attachment to solute molecules. The two-body attachment rate constants (k) obtained from the lifetime of electrons were converted to cross section as a function of the electron energy by an unfolding procedure described previously.¹⁰⁻¹²

III. RESULTS AND DISCUSSION

A. Mean electron energy dependence of rate constants

The electron attachment rate constants as a function of the mean electron energy for brominated methanes (CBr_4 , CHBr_3 , CFBr_3 , CF_2Br_2) and those containing chlorine atom(s) (CBrCl_3 , CHBr_2Cl , and CH_2BrCl) are shown in Figs. 1 and 2, respectively. CBr_4 , CFBr_3 , CF_2Br_2 , and CBrCl_3 are known to undergo dissociative attachment with no production of parent negative ions.^{6,13-16} It has been shown that the formation of Br^- and Br_2^- ions are possible for dissociative attachment to CF_2Br_2 and CFBr_3 ; the ratios of Br^- to Br_2^- are 85/15⁶ or 92/8¹⁵ for CF_2Br_2 and 90/10⁶ for CFBr_3 . In CBrCl_3 , Br^- and Cl^- ions are produced in the ratio 80/20.¹⁷ There is also evidence that both Br^- and Br_2^- are formed for CBr_4 .^{13,18} Since only the disappearance of electrons are monitored in the present measurements, the obtained rate constants correspond to total attachment processes including all the dissociation channels.

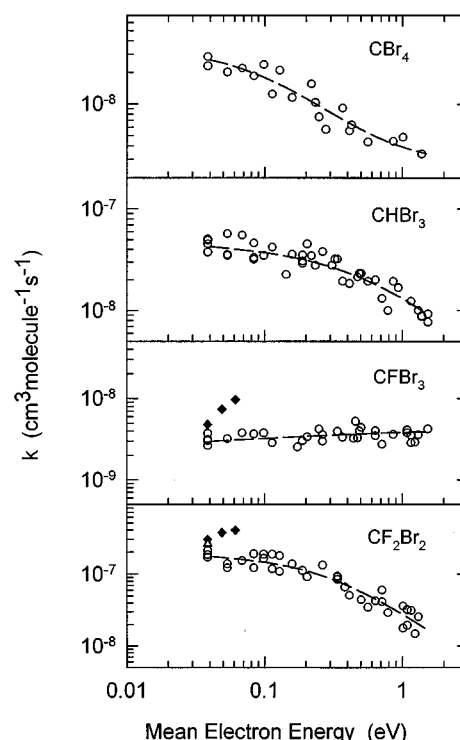


FIG. 1. Rate constants k for electron attachment to CBr_4 , CHBr_3 , CFBr_3 , and CF_2Br_2 as a function of the mean electron energy. \circ , present results; \blacklozenge , Ref. 6 (FALP technique); \triangle , Refs. 39 and 40 (electron swarm). The long dashed lines represent the values used to derive cross sections by an unfolding treatment (see text).

Most of the compounds show a peak in the rate constant at thermal energy (or probably lower than that), and the value decreases with the increase in the mean electron energy except CH_2BrCl which exhibits a peak at about 0.1 eV. The values for CFBr_3 are nearly constant over the mean electron energies varied. For some compounds the values at and near thermal energies reported by other workers are shown for comparison. The data obtained by Smith *et al.*⁶ using the flowing afterglow Langmuir probe (FALP) method for CF_2Br_2 and CFBr_3 show steeper increases in the rate constants with the mean electron energy than the present ones. Since in these data the mean electron energy has been varied by elevating the temperature of the entire gas system, the observed increase in the rate constants can be attributed to the increase in the internal (vibrational) energy of attaching molecules possessing appreciable activation energies in the reaction; for CFBr_3 the activation energy is 48 meV.⁶ These are examples of the indication that the elevation of gas temperature and that of electron temperature give different effects on the electron attachment processes.^{5,19}

The thermal electron attachment rate constants are summarized in Table I, those for CF_3Br and CH_2Br_2 were measured previously in the present laboratory and some relevant data reported by other workers are included. Although the present thermal values for CF_2Br_2 , CFBr_3 , and CBrCl_3 appear to be slightly lower than the reported values, it is uncertain whether the discrepancies are due to experimental

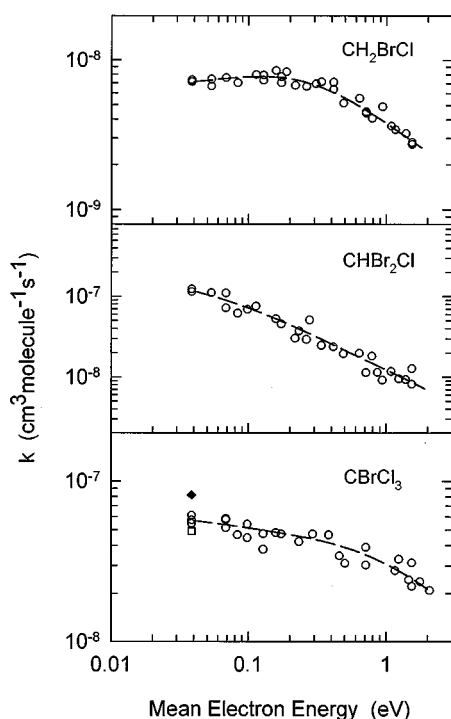


FIG. 2. Rate constants k for electron attachment to CH_2BrCl , CHBr_2Cl , and CBrCl_3 as a function of the mean electron energy. \circ , present results; \blacklozenge , Ref. 25 (FALP technique); \square , Ref. 15 (TPI intercomparison technique). The long dashed lines represent the values used to derive cross sections by an unfolding treatment (see text).

errors or some other systematic errors. In CBrCl_3 , however, if the known ratio of the production of Br^- to that of Cl^- (80:20)¹⁷ is adopted, the present value ($5.7 \times 10^{-8} \text{ cm}^3 \text{ s}^{-1}$) gives the rate constant for the Br^- formation of $4.6 \times 10^{-8} \text{ cm}^3 \text{ s}^{-1}$, which is in good agreement with a lower value $4.91 \times 10^{-8} \text{ cm}^3 \text{ s}^{-1}$ obtained by the threshold photoionization (TPI)-intercomparison technique.¹⁵

B. Electron-energy dependence of cross sections

Shown in Figs. 3–5 are the cross sections as a function of the electron energy derived by the unfolding procedure from the measured rate constants. The results for CH_2Br_2 and CF_3Br are based on the rate constant data reported previously.^{5,9} The absolute magnitude of the cross section at the peak value is listed in Table I. Since the listed cross sections corresponds to that at 0.001 eV, the values at much lower energies may be higher than that cited. In all the compounds studied the cross sections become maximum at 0 eV with no other peaks at higher energies up to about 2 eV. This seems to be common nature in the attachment to bromine-containing compounds since similar results have been obtained in brominated ethanes and ethylenes.²⁰ The absolute magnitudes of the cross sections in some compounds attain the values close to the s -wave maximum cross section $\pi\lambda^2$,^{21,22} of which energy (ϵ) dependence behaves as $\sim \epsilon^{-1}$, but in all the compounds those at very low energies behave like $\sim \epsilon^{-1/2}$. This is in accord with that predicted from a

TABLE I. Values of thermal electron attachment rate constants at room temperature and the calculated cross sections at the electron energy of 0.001 eV for brominated methanes. The values are given as, for example, 9 (–8) meaning 9×10^{-8} .

Compound	Rate constant ($\text{cm}^3 \text{ s}^{-1}$)		Cross section (cm^2) ^a
	this work	other works	
CH_3Br		7.0 (–12) ^b , 3.6 (–12) ⁱ	1.8 (–18) ^j
CH_2Br_2	9.0 ± 0.5 (–8) ^b		5.2 (–14)
CHBr_3	4.3 ± 1.0 (–8) ^a		2.7 (–14)
CBr_4	2.5 ± 0.3 (–8) ^a		1.8 (–14)
CF_3Br	8.6 ± 0.6 (–9) ^c		5.6 (–15)
CF_2Br_2	1.7 ± 0.3 (–7) ^a	3.0 (–7) ^d	1.2 (–13)
		2.6 (–7) ^e	
CFBr_3	3.0 ± 0.6 (–9) ^a	4.8 (–9) ^d	1.6 (–15)
CH_2BrCl	7.1 ± 0.2 (–9) ^a		3.6 (–15)
CHBr_2Cl	1.2 ± 0.1 (–7) ^a		1.1 (–13)
CBrCl_3	5.7 ± 0.4 (–8) ^a	8.2 (–8) ^f	3.4 (–14)
		4.91 (–8) ^g	

^aThe present work (except for CH_3Br).

^bReference 9.

^cReference 5.

^dReference 6.

^eReferences 39 and 40.

^fReference 25.

^gReference 15 (the value is for the Br formation).

^hReference 3.

ⁱReference 43.

^jReference 30 (at the electron energy of 0.38 eV).

calculation taking into account the long-range polarization of the molecule in the s -wave electron scattering developed by Klots.²³

The present cross sections have been compared with those of Br^- formation at low electron energies obtained by the threshold photoionization (TPI)¹⁵ method for CH_2Br_2 and CF_3Br and those by a high-Rydberg atom beam (HRB)¹⁶ method for CF_2Br_2 and CF_3Br . Since the TPI data do not give absolute cross sections, the values have been normalized to the rate constant at thermal energy obtained in the present study listed in Table I. The profiles of electron-energy dependence of the cross sections derived here are generally in good agreement with the TPI data. The absolute magnitude of the cross sections for CF_2Br_2 and CF_3Br obtained by the HRB method are slightly higher than the present ones. The cross section for CF_2Br_2 at 0.09 eV, the lowest accessible energy in the measurement at 393 K by electron transmission spectroscopy, is $3.3 \times 10^{-15} \text{ cm}^2$.² The present value at 0.09 eV is $8 \times 10^{-15} \text{ cm}^2$.

While CF_3Br and CH_2Br_2 lead to the formation of only a Br^- ion, CF_2Br_2 and CFBr_3 give both Br^- and Br_2^- ions. A thermochemical consideration by Zook *et al.*²⁴ has indicated that Br_2^- production is exothermic for CF_2Br_2 and CFBr_3 . Alajajian *et al.*¹⁵ have shown that the cross sections for CF_2Br_2 exhibit a peak at 0 eV for both the Br^- and the Br_2^- formation. The present result is in accord with this. Although there is no previous report on the cross sections for CFBr_3 , the present result showing only a zero-energy peak cross section corresponds to both the Br^- and the Br_2^- formation. For CBr_4 the Br^- ion is formed at 0 eV¹³ and the appearance potential of Br_2^- was measured to be 0.0 eV.¹⁸ Therefore the

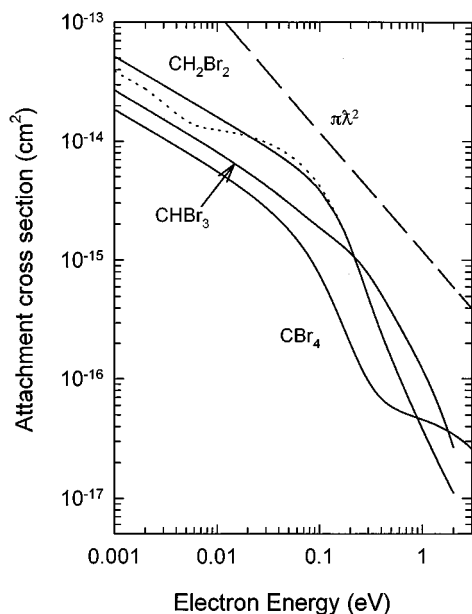


FIG. 3. Cross sections for electron attachment to CBr_4 , CHBr_3 , and CH_2Br_2 as a function of the electron energy derived by unfolding the rate constant data shown in Fig. 1 and Ref. 9. —, present results; ----, Ref. 15 (TPI); The long dashed line represents the s -wave maximum cross section $\pi\lambda^2$.

present result for CBr_4 corresponds to the formation of both Br^- and Br_2^- ions. In the attachment to CHBr_3 whether the production of Br_2^- is exothermic is uncertain since the dissociation energy of $\text{CHBr}-\text{Br}_2$ is not available. Probably the Br^- ion is the major product in this case.

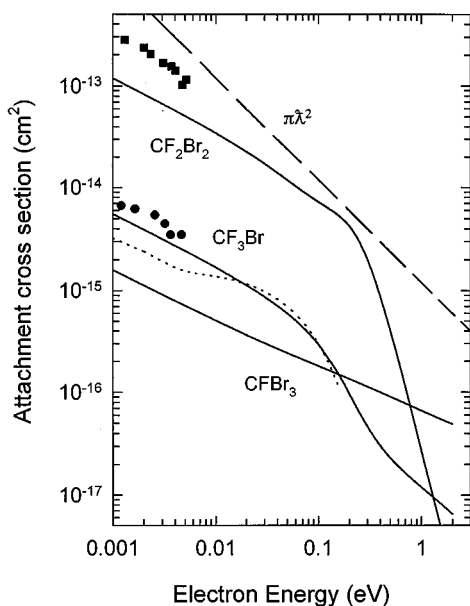


FIG. 4. Cross sections for electron attachment to CFBr_3 , CF_2Br_2 , and CF_3Br as a function of the electron energy, derived by unfolding the rate constant data shown in Fig. 1 and Ref. 5. —, present results; ----, Ref. 15 (TPI); ● (CF_2Br_2), ■ (CF_3Br), Ref. 16 (HRB). The long dashed line represents the s -wave maximum cross section $\pi\lambda^2$.

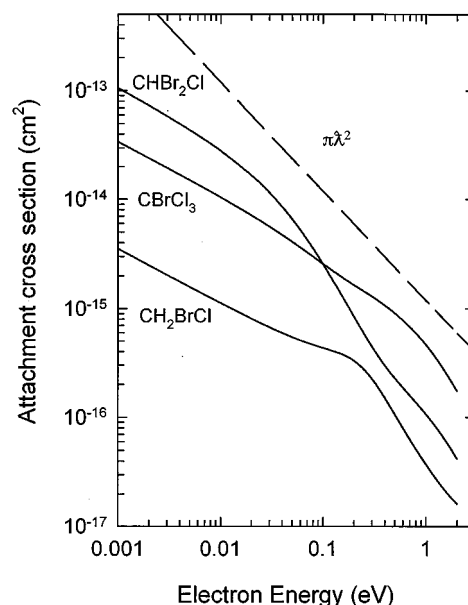


FIG. 5. Cross sections for electron attachment to CBrCl_3 , CH_2BrCl , and CHBr_2Cl as a function of the electron energy, derived by unfolding the rate constant data shown in Fig. 2. The long dashed line represents the s -wave maximum cross section $\pi\lambda^2$.

For CBrCl_3 Alajajian *et al.*¹⁵ have reported the formation of only Br^- under the single-collision condition. On the other hand, Grimsrud and Kim¹⁷ have shown that when initial electron density is smaller than the density of CBrCl_3 , the fragment negative ions formed under the condition of atmospheric pressures are Br^- (80%) and Cl^- (20%). It has also been suggested that when the initial electron density is higher than the density of CBrCl_3 , the production of the Cl^- ion increases up to 55%, due to the occurrence of electron attachment to the CCl_3 radical produced by the initial electron attachment.²⁵ Since in the present work the initial electron density is estimated to be on the order of 10^7 cm^{-3} , which is much lower than that of CBrCl_3 , $\sim 10^{11} \text{ cm}^{-3}$, employed in the measurement, the majority of the product ion may be Br^- . The formed negative ions are unknown for CH_2BrCl and CHBr_2Cl , though the formation of Cl^- and Br^- ions may be exothermic considering that the attachment to CH_2Cl_2 , CH_2Br_2 , CHCl_3 , and CHBr_3 are all exothermic.

C. Characteristics of electron attachment to brominated methanes

It has been shown by many workers that thermal rate constants for chlorinated methane increases with the number of substituted chlorine atoms, i.e., $\text{CH}_3\text{Cl} < \text{CH}_2\text{Cl}_2 < \text{CHCl}_3 < \text{CCl}_4$, and $\text{CF}_3\text{Cl} < \text{CF}_2\text{Cl}_2 < \text{CFCl}_3$. In contrast, the thermal rate constants for brominated methanes listed in Table I show a different order as $\text{CH}_3\text{Br} < \text{CBr}_4 < \text{CHBr}_3 < \text{CH}_2\text{Br}_2$ and $\text{CFBr}_3 < \text{CF}_3\text{Br} < \text{CF}_2\text{Br}_2$, indicating that a compound with two bromine atoms gives the largest rate constant (or cross sections) in each series of methanes and fluorinated methanes. The electron-energy dependence of the cross sections also show marked differences between the chlorinated

TABLE II. Resonance attachment energies E_v , the exothermicities [EA(X)-BD(R-X)], and the activation energies E_{ac} for the reaction $e^- + \text{RX} \rightarrow \text{R} + \text{X}^-$, where RX denotes a brominated methane or a chlorinated methane, and the electron affinity of RX.

RX	E_v (eV)	EA(X)-BD(R-X) ^a (eV)	E_{ac} (meV)	EA(RX) ^b (eV)
CBr ₄	~0	0.92		2.06
CHBr ₃	~0	0.52	8.7 ^g	
CH ₂ Br ₂	~0	0.47	52 ^g , 50 ^h	
CH ₃ Br	0.4 ^c	0.32	247 ^g , 300 ^h	-0.46
CFBr ₃	~0	0.9	48 ⁱ	
CF ₂ Br ₂	~0	0.7		
CF ₃ Br	~0	0.28	80 ^h	0.91
CBrCl ₃	~0	0.96		
CHBr ₂ Cl	~0			
CH ₂ BrCl	~0			
CCl ₄	~0	0.58	<0 ^g	2.12
CHCl ₃	0.3, ~0	0.17	95 ^j , 104 ^k , 139 ^g	1.70
CH ₂ Cl ₂	0.48 ^d	0.14	178 ^k , 325 ^g	1.31
CH ₃ Cl	0.8 ^d	-0.07	542 ^g	
CFCl ₃	0, 0.8	0.45	4.3 ^g	1.1
CF ₂ Cl ₂	0.3 ^e , 0.8 ^{e,f}	0.32	147 ^g , 195 ^l	0.4
CF ₃ Cl	1.5 ^{e,f}	-0.11	247 ^g	-0.4

^aThe dissociation energy is obtained from values of the heat of formation (Ref. 44) using the relation $\text{BD}(\text{R}-\text{X}) = H_f(\text{R}) + H_f(\text{X}) - H_f(\text{RX})$. EA(Br)=3.36 eV and EA(Cl)=3.62 eV. In the energetic consideration only the formation of the Br⁻ ion is considered in the bromine-containing methanes.

^bReference 45.

^cReference 30.

^dReference 26.

^eReference 2.

^fReference 7.

^gReference 31.

^hReference 32.

ⁱReference 6.

^jReference 21.

^kReference 46.

^lReference 47.

and brominated methanes. For the chlorinated compounds the peak cross sections producing Cl⁻ ions located at relatively high energies and the energy decreases as the number of chlorine atom; CH₃Cl (0.80 eV),²⁶ CH₂Cl₂ (0.48 eV),²⁶ CHCl₃ (0, 0.27 eV),²⁶ and CCl₄ (~0 eV),^{26,27} and also CF₃Cl (1.5 eV),^{2,7} CF₂Cl₂ (0.3, 0.8 eV),^{2,7} (0.3 eV),² and CFCl₃ (~0 eV)^{27,28} (see Table II). In contrast, Br-containing compounds all give maximum cross sections at 0 eV, as shown in Figs. 3–5. A distinct feature of the brominated methanes can be seen by comparing the cross sections for CBr₄, CHBr₃, and CFBr₃ with those for the corresponding chlorinated compounds CCl₄, CHCl₃, and CFCl₃ shown in Figs. 8–10 in the Appendix. CCl₄ and CFCl₃ give peak cross sections at zero energy, and CHCl₃ exhibits the peak at the electron energy of 0.3 eV, with the absolute magnitude $\text{CHCl}_3 < \text{CFCl}_3 < \text{CCl}_4$, while the corresponding brominated methanes all show a zero-energy peak of the cross sections with the magnitude $\text{CFBr}_3 < \text{CBr}_4 < \text{CHBr}_3$.

The profile and the magnitude of the cross sections for the dissociative attachment can be interpreted in terms of relative location of diatomiclike potential-energy curves be-

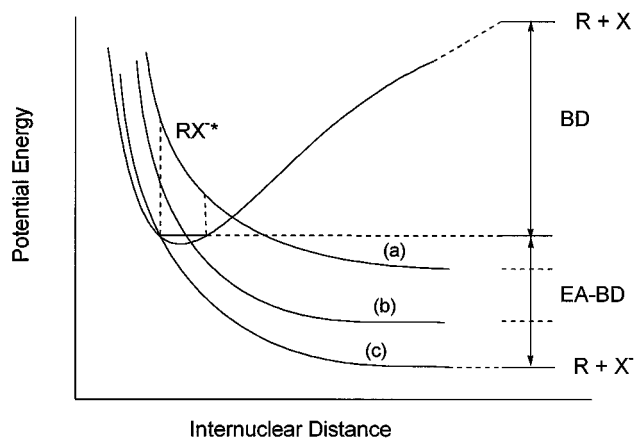


FIG. 6. Schematic representation of the potential energy for dissociative electron attachment to the halogen-containing compound RX. BD is the dissociation energy of bond R-X, and EA is the electron affinity of halogen atom X. The value of EA-BD represents the exothermicity of the reaction for zero-energy electrons. The electron attachment occurs vertically, and the unstable negative-ion RX^* dissociates along the repulsive potential energy curves (a), (b), and (c), depending upon the value of EA-BD, in competition with the autodetachment of the electron from RX^* .

tween a neutral molecule (attractive) and the corresponding negative ion (repulsive). Typical potential energy curves are shown in Fig. 6. The position of the repulsive ion potential relative to that of the neutral may be determined by the bond-dissociation energy (BD) and the electron affinity (EA) of the halogen atom that dissociates. Note that in the negative-ion potential the existence of a minimum, if there is, is neglected for simplicity. When EA-BD is positive the attachment reaction for a zero-energy electron is exothermic, and the larger EA-BD, the more exothermic; the values of EA-BD for relevant chloromethanes and bromomethanes are listed in Table II. The change in the value of EA-BD may be reflected on the relative positions between the neutral and ionic potentials in the Franck-Condon region. One can claim that the electron affinity of the parent molecule could be a measure of the relative position between the neutral and ionic potentials (the values of EA for the parent molecules are listed in Table II, though limited values are known for the brominated methanes). However, the EA values determine the relative position between the minimum of the neutral potentials and that of the ion potential, and do not predict the relative position in the Franck-Condon region. For example, $\text{EA}(\text{CHCl}_3) > \text{EA}(\text{CH}_2\text{Cl}_2) > \text{EA}(\text{CFCl}_3)$, yet CFCl₃ capture electrons very efficiently with the resonance attachment energy at 0 eV, while the attachment cross sections for CHCl₃ and CH₂Cl₂ are rather small and their resonance energies are located above 0 eV. More useful quantities in the prediction of the relative position of the potential curves should be the resonance attachment energy and the activation energy for the reaction, the importance of which will be discussed in a later section. For the moment we consider only the exothermicity (EA-BD) for a qualitative discussion.

For chlorinated methanes the value of BD for an R-Cl bond decreases with the number of Cl atoms in the molecule.

The potential-energy curve of the negative ion becomes lower with the number of Cl atoms, from curve (a) to curve (b). Thus the resonance energy for the electron attachment decreases with the number of Cl atoms. At lower resonance energy the absolute magnitude of the cross sections becomes larger because the survival probability against the autodetachment of an electron from the ion increases. These are consistent with the experimental observation for the cross sections of chlorinated methanes. Similarly, for brominated methanes CF_xBr_y ($x+y=4$), as the number of Br atoms increases the value of BD decreases slightly. In all the brominated methanes the cross sections become the maximum at 0 eV. This implies that the potential-energy curve of the negative ion crosses near the equilibrium position of the neutral potential-energy curve. If we regard that curve (b) corresponds to CF_2Br_2 , the cross sections for CFBr_3 might become even larger than those of CF_2Br_2 . However, the present experimental results show much smaller cross sections for CFBr_3 than those for CF_2Br_2 . To explain this one may propose that in CFBr_3 the potential-energy curve for the ion becomes much like the curve (c) which is so low that the crossing point of the ion curve is at a shorter internuclear distance than the equilibrium distance of the neutral and the probability of the transition from the neutral to the ion becomes lower than the curve (b). This may be similar to the “inverted region” of the electron transfer rate constant in the charge recombination in solution proposed by Marcus.²⁹ In curve (c) the activation energy can still exist and is regarded as the vertical energy at the crossing point. An appreciable amount of activation energy of 48 meV reported for the electron attachment to CFBr_3 (Ref. 6) may correspond to this.

The change in the magnitude of the cross sections when one of the chlorine atoms in a chlorinated methane is substituted by a bromine atom is interesting in the light of the above consideration. For example, the relative magnitude in the cross sections varies as (i) $\text{CH}_2\text{Br}_2 > \text{CH}_2\text{BrCl} > \text{CH}_2\text{Cl}_2$ and (ii) $\text{CCl}_4 > \text{CBrCl}_3 > \text{CBr}_4$. The introduction of a bromine atom lowers the potential energy for the negative ion. Therefore in the inequality (i), CH_2Br_2 corresponds to the potential-energy type (b) and by going from it to CH_2BrCl to CH_2Cl_2 the energy successively increases, giving smaller cross sections. In the case of (ii), CCl_4 is already in the type (b) and the introduction of a Br atom further lowers the energy to give the type (c) of which cross sections are smaller than the type (b). With further substitution of Cl with Br atoms, as in CBr_4 , the potential-energy curve becomes an extreme case of the type (c), which gives even smaller cross sections.

One can propose similar interpretation for the cross sections in the CH_xBr_y series, which indicates $\text{CH}_3\text{Br} \ll \text{CBr}_4 < \text{CHBr}_3 < \text{CH}_2\text{Br}_2$. Indeed a very low rate constant for CH_3Br corresponds to its cross-sections peak at about 0.4 eV.³⁰ The inequality $\text{CBr}_4 < \text{CHBr}_3 < \text{CH}_2\text{Br}_2$, all showing peak cross sections at zero energy, can be explained by the fact that the potential-energy for the CBr_4^- and CHBr_3^- ions corresponds to the curve (c) with CBr_4^- lower than CHBr_3^- . However, there is a crucial difficulty in this case. The temperature dependence measurement for CHBr_3 shows a low

activation energy of 8.7 meV,³¹ which is much lower than that for CH_2Br_2 (52, 50 meV)^{31,32} (see Table II). Such a low activation energy would give a high rate constant even for the potential-energy curve (c). This contradicts the observation. Thus there must be other factors which control the attachment processes.

The potential-energy curves in Fig. 6 are drawn along the C–Br internuclear distance assuming a diatomiclike molecule, simply because the dissociation channel is important in the attachment. However, the real potential energies for the neutral and negative-ion states should be composed of a multidimensional surface taking into account whole conformation of the molecule. Let us consider the attachment to CHBr_3 . Based on the infrared and Raman data³³ the CHBr_3 molecule possesses fundamental vibrational modes associated with CBr_3 deformation (the vibrational energy of 0.019 and 0.027 eV, e and a_1 symmetry, respectively) and CBr stretching (0.066 and 0.080 eV for a_1 and e , respectively). Thus even at room temperature the CBr_3 deformation mode is in the excited state. The FALP study has suggested that the electron attachment to the CCl_3 radical is very effective with the rate constant at 300 K being $2.4 \times 10^{-7} \text{ cm}^3 \text{ s}^{-1}$.²⁵ Recently it has been suggested that in the electron attachment to CHCl_3 the attachment to the local CCl_3 group in the vibrationally excited state is strongly enhanced at an elevated temperature.³⁴ Although the CBr_3 radical and the CBr_3 group in the CHBr_3 molecule may not be the same, the latter behaves much like the former as in the CCl_3 group in CHCl_3 . As the electron affinity of the CBr_3 radical is $\sim 1.8 \text{ eV}$,³⁵ the formation of CBr_3^- is likely. These considerations lead to the model that the initial electron attachment occurs in the CHBr_3 molecule in the negative-ion state in which the CBr_3 deformation mode is vibrationally excited, and the subsequent dissociation occurs in the C–Br stretching mode, as depicted in Fig. 7. The reaction coordinate for the dissociative attachment process involves, instead of direct transition to antibonding σ^* (C–Br) orbital, the transition to the potential-energy surface primarily corresponding to the CBr_3^- radical anion, followed by the elongation of one of the three C–Br bonds to lead its dissociation. In this case, the activation energy corresponds to the energy at which the CBr_3^- ion state crosses over to that of the coordinate in the C–Br stretching mode, and the attachment cross sections still reflect the potential energy surface at the Franck–Condon region in the initial attachment to the CBr_3 group. This type of electron attachment may also be true of CBr_4 which has vibrational frequencies even lower than CHBr_3 . Furthermore, we can extend similar interpretation to the dissociative attachment to other compounds which have appreciable activation energies but show a zero-energy peak in the cross sections. As far as the diatomiclike potential as shown in Fig. 6 is considered, the electron attachment showing a zero-energy peak cross section should not give an appreciable activation energy. Most of the brominated compounds studied so far have appreciable activation energies, as listed in Table II, yet show a zero-energy peak in the cross sections. Thus we can extend the interpretation as made in Fig. 7 to the dissociative attachment to all those brominated com-

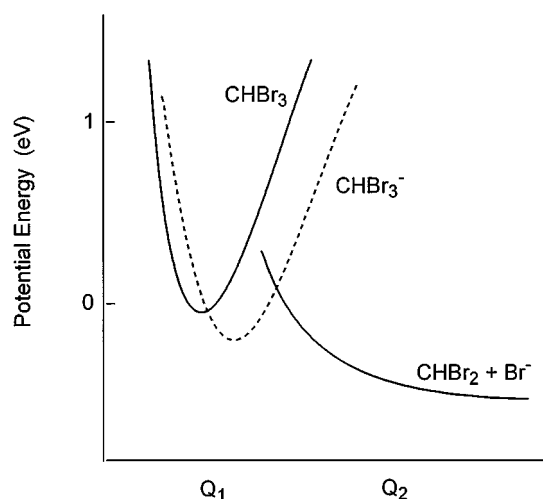


FIG. 7. Schematic representation of the potential energy for dissociative electron attachment to CHBr_3 . Q_1 and Q_2 represent different motions in the ion or the reaction coordinate. The electron attachment occurs initially on the coordinate Q_1 and the formed ion undergoes a transition to the coordinate Q_2 resulting in the bond dissociation. In the drawing the resonance attachment energy (0 eV) and the activation energy (8.7 meV) for the reaction have been taken into account.

pounds. The extent of the contribution of a local brominated group to the initial attachment may depend on the specific structure, namely the numbers of bromine, chlorine, and fluorine atoms in the compound. The occurrence of unimolecular production of Br_2^- found in thermal electron attachment to CF_2Br_2 and CFBr_3 may well be understood by initial attachment to the Br_2 and Br_3 groups, respectively.

IV. CONCLUSION

The low-energy electron attachment to brominated methanes, especially to those containing two or more Br atoms, is not interpreted as in the corresponding chlorinated methanes. All the brominated compounds including methanes, ethanes, and ethylenes show peak cross sections at zero electron energy. A collective nature of bromine atoms in a molecule plays an important role in the electron capture property. It may be due to the large size of the bromine atom, much stronger interaction with free electrons, and weaker strength of the C–Br bond compared with the corresponding chlorinated compounds. For iodinated methanes we can suggest a similar or even stronger effect of such “unusual” properties in the low-energy electron attachment.

ACKNOWLEDGMENTS

This work was supported partly by a Grant-in-Aid for Scientific Research on Science of Free Radicals in Priority Areas from the Ministry of Education, Science, Sports and Culture, Japan.

APPENDIX

In order to acquire better understanding of the nature of the electron attachment to brominated methanes, we have

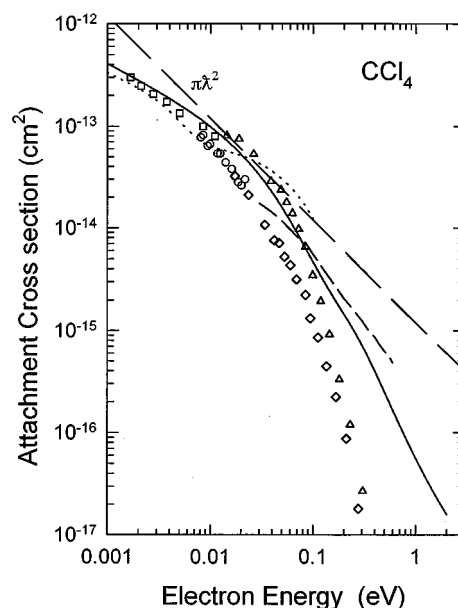


FIG. 8. Cross sections for electron attachment to CCl_4 as a function of the electron energy derived by unfolding the rate constant data shown in Ref. 5. —, present result; ----, Ref. 27 (TPI); - · - ·, Ref. 36 (electron swarm); ○, Ref. 37 (HRB); □, Ref. 37 (HRB); △, Ref. 41 (HRB); ◆, Ref. 41 (HRB); The long dashed line represents the s -wave maximum cross section πk^2 .

presented newly derived cross sections for electron attachment to CCl_4 , CFCl_3 , and CHCl_3 (Figs. 8–10). These values have been calculated using the unfolding method from data of rate constants as a function of the mean electron energy

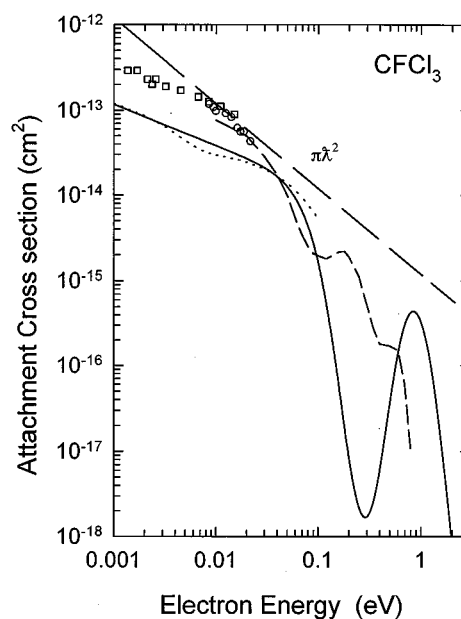


FIG. 9. Cross sections for electron attachment to CFCl_3 as a function of the electron energy derived by unfolding the rate constant data shown in Ref. 5. —, present result; ----, Ref. 27 (TPI); - · - ·, Ref. 28 (electron swarm); ○, Ref. 37 (HRB); □, Ref. 37 (HRB); The long dashed line represents the s -wave maximum cross section πk^2 .

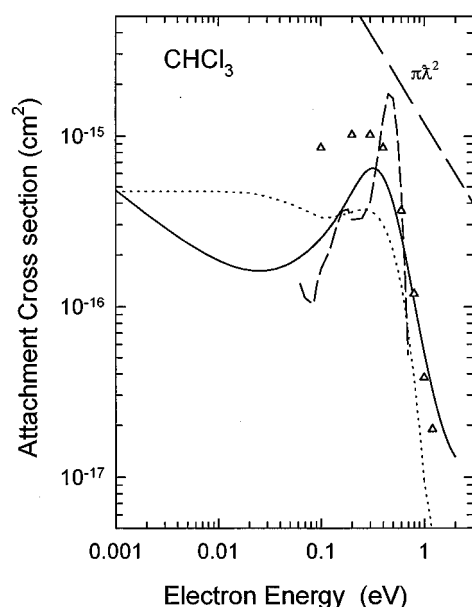


FIG. 10. Cross sections for electron attachment to CHCl_3 as a function of the electron energy derived by unfolding the rate constant data shown in Ref. 5. —, present results; ----, Ref. 28 (electron swarm); Δ , Ref. 42 (electron beam); - · -, Ref. 26 (electron beam). The long dashed line represents the s -wave maximum cross section $\pi\lambda^2$.

reported previously. The results are shown along with other previous data. In CCl_4 the cross sections tend to have the maximum at 0 eV and become very close to those expected for s -wave electrons ($\pi\lambda^2$). The cross sections for CCl_4 are in good agreement with most of the previous data.^{27,36,37} Two peaks at 0 and 0.8 eV are apparent in the dissociative attachment to CFCl_3 . The peak at 0 eV corresponds to the Cl^- formation and that at 0.8 eV may be the production of the Cl_2^- ion, which is in accord with the result of the electron impact study.⁷ The peak at 0.3 eV in CHCl_3 also corresponds to the Cl^- production. An increase in the cross sections as the electron energy decreases to zero may be real.^{26,38}

¹For example, L. G. Christophorou, D. L. McCorkle, and A. A. Christodoulides, *Electron-Molecular Interactions and Their Applications*, edited by L. G. Christophorou (Academic, New York, 1984), Vol. 1, Chap. 6; T. Oster, A. Kühn, and E. Illenberger, *Int. J. Mass Spectrom. Ion Proc.* **89**, 1 (1989); D. Smith and P. Španěl, *Adv. At. Mol. Opt. Phys.* **32**, 307 (1994).

²T. Underwood-Lemons, T. J. Gergel, and J. H. Moore, *J. Chem. Phys.* **102**, 119 (1995).

³K. M. Bansal and R. W. Fessenden, *Chem. Phys. Lett.* **15**, 21 (1972).

⁴R. W. Fessenden and K. M. Bansal, *J. Chem. Phys.* **53**, 3468 (1970).

⁵H. Shimamori, Y. Tatsumi, Y. Ogawa, and T. Sunagawa, *J. Chem. Phys.* **97**, 6335 (1992).

⁶D. Smith, C. R. Herd, N. G. Adams, and J. F. Paulson, *Int. J. Mass Spectrom. Ion Proc.* **96**, 341 (1990).

⁷E. Illenberger, *Ber. Bunsenges. Phys. Chem.* **86**, 252 (1982).

⁸H.-U. Scheunemann, E. Illenberger, and H. Baumgärtel, *Ber. Bunsenges. Phys. Chem.* **84**, 580 (1980).

⁹H. Shimamori, Y. Tatsumi, Y. Ogawa, and T. Sunagawa, *Chem. Phys. Lett.* **194**, 223 (1992).

- ¹⁰L. G. Christophorou, D. L. McCorkle, and V. E. Anderson, *J. Phys. B* **4**, 1163 (1971).
- ¹¹H. Shimamori, T. Sunagawa, Y. Ogawa, and Y. Tatsumi, *Chem. Phys. Lett.* **227**, 609 (1994).
- ¹²H. Shimamori, T. Sunagawa, Y. Ogawa, and Y. Tatsumi, *Chem. Phys. Lett.* **232**, 115 (1995).
- ¹³J. K. Olthoff, J. H. Moore, and J. A. Tossell, *J. Chem. Phys.* **85**, 249 (1986).
- ¹⁴R. S. Mock, D. R. Zook, and E. P. Grimsrud, *Int. J. Mass Spectrom. Ion Proc.* **91**, 327 (1989).
- ¹⁵S. H. Alajajian, M. T. Bernius, and A. Chutjian, *J. Phys. B* **21**, 4021 (1988).
- ¹⁶A. Kalamarides, R. W. Marawar, X. Ling, C. W. Walter, B. G. Lindsay, K. A. Smith, and F. B. Dunning, *J. Chem. Phys.* **92**, 1672 (1990).
- ¹⁷E. P. Grimsrud and S. H. Kim, *Anal. Chem.* **51**, 537 (1979).
- ¹⁸J. J. DeCorpo and J. L. Franklin, *J. Chem. Phys.* **54**, 1885 (1971).
- ¹⁹D. Smith, C. R. Herd, and N. G. Adams, *Int. J. Mass Spectrom. Ion Proc.* **93**, 15 (1989).
- ²⁰T. Sunagawa and H. Shimamori, *Int. J. Mass Spectrom. Ion Proc.* **149/150**, 123 (1995).
- ²¹J. M. Warman and M. C. Sauer, Jr., *Int. J. Radiat. Phys. Chem.* **3**, 273 (1971).
- ²²A. A. Christodoulides, L. G. Christophorou, R. Y. Pai, and C. M. Tung, *J. Chem. Phys.* **70**, 1156 (1979).
- ²³C. E. Klotz, *Chem. Phys. Lett.* **38**, 61 (1976).
- ²⁴D. R. Zook, W. B. Knighton, and E. P. Grimsrud, *Int. J. Mass Spectrom. Ion Proc.* **104**, 63 (1991).
- ²⁵N. G. Adams, D. Smith, and C. R. Herd, *Int. J. Mass Spectrom. Ion Proc.* **84**, 243 (1988).
- ²⁶S. C. Chu and P. D. Burrow, *Chem. Phys. Lett.* **172**, 17 (1990).
- ²⁷O. J. Orient, A. Chutjian, R. W. Crompton, and B. Cheung, *Phys. Rev.* **39**, 4494 (1989).
- ²⁸D. L. McCorkle, A. A. Christodoulides, L. G. Christophorou, and I. Szamrej, *J. Chem. Phys.* **72**, 4049 (1980); **76**, 753E (1982).
- ²⁹R. A. Marcus, *Annu. Rev. Phys. Chem.* **15**, 155 (1964).
- ³⁰P. G. Datskos, L. G. Christophorou, and J. G. Carter, *J. Phys. Chem.* **97**, 9031 (1992).
- ³¹E. C. M. Chen, K. Albyn, L. Dussack, and W. E. Wentworth, *J. Phys. Chem.* **93**, 6827 (1989).
- ³²E. Alge, N. G. Adams, and D. Smith, *J. Phys. B* **17**, 3827 (1984).
- ³³G. Herzberg, *Molecular Spectra and Molecular Structure, II. Infrared and Raman Spectra of Polyatomic Molecules* (Van Nostrand, Princeton, 1954), Chap. III.3.
- ³⁴T. Sunagawa, Ph.D. thesis submitted to Fukui Institute of Technology, 1997.
- ³⁵F. M. Page and G. C. Goode, *Negative Ions and the Magnetron* (Wiley, New York, 1969).
- ³⁶A. A. Christodoulides and L. G. Christophorou, *J. Chem. Phys.* **54**, 4691 (1971).
- ³⁷F. B. Dunning, *J. Phys. Chem.* **91**, 2244 (1987).
- ³⁸D. Spence and G. J. Schulz, *J. Chem. Phys.* **58**, 1800 (1973).
- ³⁹T. G. Lee, *J. Phys. Chem.* **67**, 360 (1963).
- ⁴⁰R. P. Blaunstein and L. G. Christophorou, *J. Chem. Phys.* **49**, 1526 (1968).
- ⁴¹K. Harth, M.-W. Ruf, and H. Hotop, *Z. Phys. D* **14**, 149 (1989).
- ⁴²H.-X. Wan, J. H. Moore, and J. A. Tossell, *J. Chem. Phys.* **94**, 1868 (1991).
- ⁴³K. G. Mothes, E. Schultes, and R. N. Schindler, *J. Chem. Phys.* **76**, 3758 (1972).
- ⁴⁴*CRC Handbook of Chemistry and Physics*, 65th ed., edited by R. C. Weast (CRC Press, Boca Raton, FL, 1984).
- ⁴⁵A. A. Christodoulides, D. L. McCorkle, and L. G. Christophorou, *Electron-Molecular Interactions and Their Applications*, edited by L. G. Christophorou (Academic, New York, 1984), Vol. 2, Chap. 6.
- ⁴⁶E. Schultes, A. A. Christodoulides, and R. N. Schindler, *Chem. Phys.* **8**, 354 (1975).
- ⁴⁷R. Schumacher H.-R. Sprünken, A. A. Christodoulides, and R. N. Schindler, *J. Phys. Chem.* **82**, 2248 (1978).